

## A Dynamic Model with Structured Recurrent Neural Network to Predict Glucose-Insulin Regulation of Type 1 Diabetes Mellitus

Hsiao-Ping Huang,\*<sup>†</sup> Shih-Wei Liu,\*  
I-Lung Chien,\*\* Chia-Hung Lin\*\*\*

\* *Department of Chemical Engineering, National Taiwan University, Taipei 106, Taiwan*  
<sup>†</sup> (Tel: 886-2-23638999; e-mail: huanghpc@ntu.edu.tw)

\*\* *Department of Chemical Engineering, National Taiwan University of Science and Technology, Taipei 106, Taiwan*

\*\*\* *Endocrinology and Metabolism, Department of Internal Medicine, Chang Gung Memorial Hospital, Tao-Yuan, Taiwan*

---

**Abstract:** An artificial neural network (ANN) model for the prediction of glucose concentration in a glucose-insulin regulation system for type 1 diabetes mellitus is developed and validated by using the Continuous Glucose Monitoring System (CGMS) data. This network consists of structured framework according to the compartmental structure of the Hovorka-Wilinska model (HWM), and an additional update scheme is also included, which can improve the prediction accuracy whenever new measurements are available. The model is tested on a real case, as well as long term prediction has been carried over an extended time horizon from 30 minutes to 4 hours, and the quality of prediction is assessed by examining the values of the four indexes. For instant, the overall Clarke error grid (CEG) Zone A value is up to 100% for the 30-min-ahead prediction horizon with update. Therefore, for practical purpose, our results indicate that the promising prediction performance can be achieved by our proposed structured recurrent neural network model (SRNNM).

*Keywords:* type 1 diabetes, neural network

---

### 1. INTRODUCTION

Diabetes mellitus is one of the most common metabolic diseases characterized by an incapability to control blood glucose concentration in the body, and there exist two basic types of diabetes mellitus, including type 1 and type 2. Particularly, type 1 diabetes mellitus (T1DM) is caused by failure of the pancreas to secrete insulin due to the autoimmune destruction of the pancreatic islet  $\beta$ -cells. Therefore, the patients with T1DM must rely on daily insulin injections/infusions for the regulation of blood glucose, i.e., insulin-dependent diabetes mellitus (IDDM). Those daily injections/infusions, insulin therapies, artificially mimic the endogenous insulin secretion presenting in normal human bodies to maintain their blood glucose (BG) levels within an acceptable range. This mimic mechanism can be attained to a certain degree by continuous subcutaneous insulin infusion (CSII) with an insulin pump, which administers continuous basal insulin infusion rate and prandial insulin boluses. However, based on infrequent subcutaneous BG measurements, this administration of such insulin infusions to prevent hyperglycemia and hypoglycemia and to maintain BG at an acceptable level is still an issue, especially when the patient has irregular diets or activities. Recently, the CGMS has been a commercialized device which can provide maximal information about BG levels throughout a long period of time and can facilitate physicians to make optimal therapy recommendations for the patients with T1DM.

For the improvement of insulin therapies, currently, a number of model-based glucose-insulin regulation systems have been developed and can be used to analyze past therapies, to predict future BG levels and to give therapy recommendations. So far, those systems are either based on physiological or empirical models. One of the pioneering papers in this field is Bolie (1961), and the author proposed a physiology simple model. However, the real beginning of modelling glucose-insulin dynamics started with the so-called minimal model. (Toffolo et al., 1980) (Bergman, 2003) The authors stated that minimal model made a few assumptions that may not be necessary or realistic. Another more common ODE model was developed Hovorka et al. (2004) and then modified by his co-workers. (Wilinska et al., 2005) Man et al. (2007) presented a more complicated simulation model in normal humans that describes the physiological dynamics that occur after a meal. In addition, Sorensen et al. (1985) developed another complicated physiology models, which describes biochemical species dynamics at each significant organ site. On the other hand, the other type of model-based systems, empirical models, includes dynamic input-output models and neural networks. Among dynamic input-output models, generally, autoregressive exogenous input (ARX) models were widely used. (Bellazzi et al., 1995) Autoregressive moving average exogenous input (ARMAX) models are similar to ARX models but describe the prediction errors as moving averages of noise. (Finan et al., 2009) By comparison between those two kinds of empirical models, neural networks have emerged as techniques that can potentially deal with complicated biological problems, for

example, the highly nonlinear and individual-specific dynamics of insulin-glucose regulation systems. (Trajanoski and Wach, 1998) have used neural networks to identify a nonlinear ARX (NARX) model in simulation study. Tresp et al. (1999) studied the application of neural networks and compared the performance for two different types of neural networks. Mougiakakou et al. (2005) proposed a system based on the combination of compartmental models and neural networks, and validated by the data from invasive finger lacing test. Despite that the aforementioned mathematical models have been reported, there is still a need for on-line long term prediction model for implementing real-time control and forecasting hypo/hyper-glycemia by using the CGMS data which can provide maximal information. In this work, we proposed a prediction model with a structured neural network, and this model was identified and validated by the CGMS data from patients with T1DM who have regular meals and insulin dosages. Furthermore, an additional update scheme is also embedded in our model so that the multi-steps ahead prediction can be updated whenever new measurements are available.

## 2. DEVELOPMENT OF PREDICTION MODEL

In general, development of empirical or semi-empirical models for a dynamic system needs sufficient excitations to the system. Nevertheless, sufficient excitations cannot be arbitrarily applied to a human body, especially who has T1DM. Also for a system with high order dynamics and high nonlinearity, conventional black-box approach could not yield a good model for long-term prediction. Upon the above considerations, a physical model is required, and neural net models are then used to realize this physical model for prediction purposes. In this work, the model developed by Hovorka et al. (2004) and modified by Wilinska et al. (2005) is selected, because it has a reasonable trade-off between simplicity and physiology. Briefly, this nonlinear model consists of a glucose subsystem, an insulin subsystem, and an insulin action subsystem. An additional factor of this model is that it can describe nonlinearity because of both the insulin actions and physiological-based saturation effects. In the following sections, this model will be referred to as the Hovorka-Wilinska model (HWM). Because the HWM totally has nine ordinary differential equations, it would encounter difficult initialization steps, if the time origin is required to be able to move arbitrarily for practical on-line implementation purpose. In comparison, our proposed ANN model can reduce those difficult steps. The data from sufficient excitations on the identified HWM to can be used for ANN model training, and those sufficient data can avoid model overfitting. In addition, the compensation RNN (Recurrent Neural Network) to take care of the discrepancy between the HWM data and the CGMS data from the real patient is constructed and embedded in our model. In the following, we will briefly demonstrate the identification of the HWM and the model with structured RNN are briefly introduced.

### 2.1 The identification of the HWM

The detailed equations of the HWM are given in Appendix A. In this model, totally, there are fourteen parameters which must be determined for each specific patient. They are,

$$p = \left\{ \begin{array}{l} E_{01}, k_{12}, EGP_0, k_{a1}, k_{a2}, k_{a3}, S_{IT}^f, S_{ID}^f, S_{IE}^f \\ V_{max,LD}, k_{M,LD}, k_e, k_{a1*}, k_{a2*} \end{array} \right\}$$

Firstly, we assumed that the insulin dosages and the content of each meal provided from a diary and the BG data collected by the CGMS are accurate during an experimental period. Using only those first two days of the data, the parameters of the HWM are then identified to fit the data by minimizing the objective function given in (1).

$$J = \phi \left\{ \sum_{t=t_i}^{t_f} [G(t) - \tilde{G}(t)]^2 \right\} + |S_f^0 - S_f(p)| \quad (1)$$

where  $\phi$  is the weight,  $t_i$  is the initial time of experiment period,  $t_f$  is the final time of the data,  $G(t)$  are the measurements recorded on the CGMS,  $\tilde{G}(t)$  is computed by integrating the HWM,  $S_f^0$  is the targeting fasting level value taken as pre-breakfast (one hour) average in the data set, and  $S_f(p)$  is the fasting level obtained from the HWM. The latter term in this objective function is added for the purpose of increasing the physiological feasibility, and this term is given as zero if the  $S_f(p)$  value is within the tolerant range.

In addition, the Simulated Annealing (SA) optimal algorithm was adopted to search the optimal parameters because this algorithm has more potential for finding the global minimum of the objective function instead of the local minimum. The initial guess of those parameters was taken from the literatures (Hovorka et al., 2004, Wilinska et al., 2005), and the initial conditions of the state variables were calculated by solving the nonlinear algebraic equations. Next, several experiments were conducted for determining the adopted algorithm parameters (e.g., the initial temperature, temperature decrement). After fitting the model to CGMS data, we assumed the lack of fit in the extending time horizon is due to imprecise quantification of carbohydrate intakes and different intake or digestion durations for each meal. We slightly modified the carbohydrate intakes (<5%), and searched the acceptable  $t_{max,G}$  value of each meal.

### 2.2 Prediction model with structured RNN

Based on the HWM, these identified parameters generate data for neural network training. A prediction model with structured RNN was developed based on the structure of this compartmental physiological HWM. A block diagram of our proposed SRNNM is shown in Fig. 1 and Fig. 2. The two inputs in this model are meal ( $u_1 = \{D_G, t_{max,G}\}$ ) and insulin ( $u_2 = \{u_{basal}, u_{bolus}\}$ ). As can be seen, the sub-RNN for  $q_3$  was constructed to mimic the dynamic response of  $q_3$  from (17) - (20) in Appendix A. Similarly, sub-RNNs for  $x_1$ ,  $x_2$ , and  $x_3$  were constructed to describe the dynamic behaviour from (14), (15), and (16), respectively in Appendix A. Then, RNN for  $Q_1$  &  $Q_2$  was constructed for (8) and (9) in Appendix A. After that, an additional sub-RNN to compensate for the bias between  $\tilde{G}(t)$  and the CGMS data  $G(t)$  due to the insufficient dynamic description in the HWM was also constructed. To be specific,

$$G(t) = \tilde{G}(t) + \delta_1(\tilde{G}, Q_2, x_1, x_3, U_G) + \delta_2(\tilde{G}(t) + \delta_1(\tilde{G}, Q_2, x_1, x_3, U_G) = f(\tilde{G}, Q_2, x_1, x_3, U_G) = \hat{G}(t) \quad (2)$$

where  $\delta_1$  is referred to as the bias related to the insufficiency in the HWM, and  $\delta_2$  is the residual of the model fit. By combining these sub-networks, a prediction network was constructed.

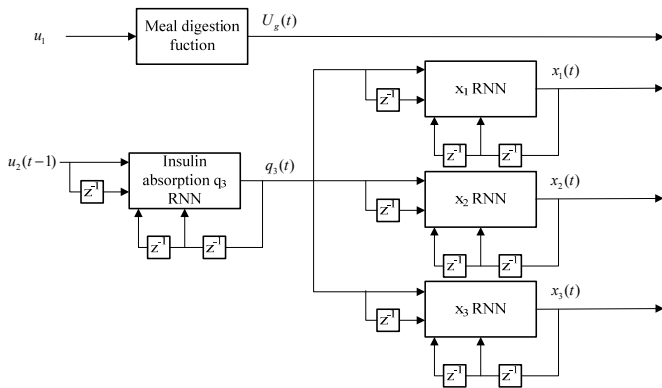


Fig. 1. The first part of the SRNNM.

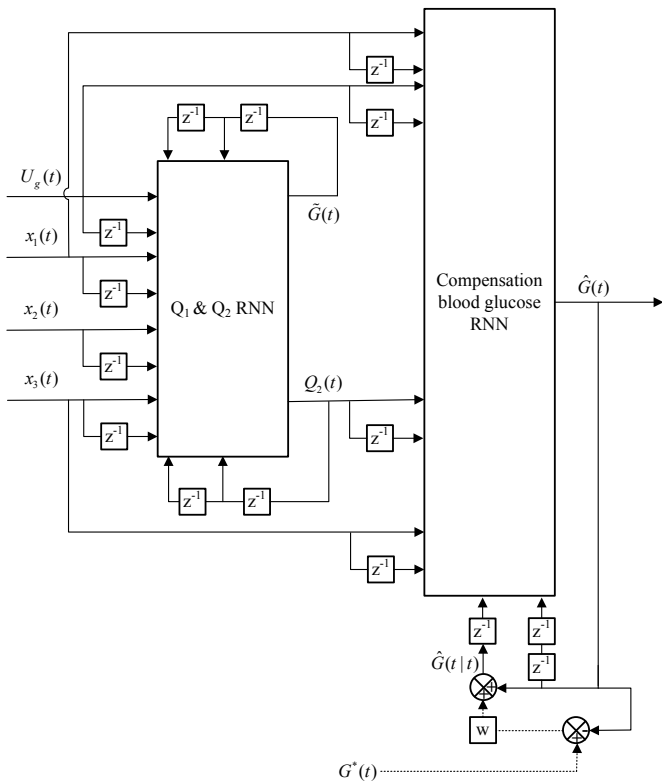


Fig. 2. The second part of the SRNNM.

### 2.3 New available measurements update scheme

In addition, we designed an update scheme to improve the performance of prediction whenever new measurements are available. As shown in Fig. 1 and Fig. 2, when the blood glucose was reported by a new infrequent measurement (i.e.,

$G^*(t)$ ), the difference between  $G^*(t)$  and  $\hat{G}(t)$  was weighted, then added to  $\hat{G}(t)$  to estimate  $\hat{G}(t|t)$ .

## 3. PREDICTION AND ACCURACY OF THE MODEL

### 3.1 Long term prediction

The following prediction horizons were employed in this work (sampling time: 5 min): 6-step-ahead (30-min-ahead), 24-step-ahead (2-hr-ahead), and 48-step-ahead (4-hr-ahead).

Firstly, the uncorrected prediction of BG (i.e.,  $\hat{G}(t|t-1)$ ) was obtained from implementing the SRNNM that consists of Fig. 1 and Fig. 2. By recursive use of this model, the prediction of BG can be computed along the extended time in the future, i.e.,  $\hat{G}(t+i|t-1); i=1,2,\dots,N$ .

The predictive BG can be refreshed whenever new measurement of BG is available to work the update scheme in a manner of the following:

$$\hat{G}(t|t) = \hat{G}(t|t-1) + w[G^*(t) - \hat{G}(t|t-1)] \quad (3)$$

The appropriate proportional weight  $w$  can be obtained by optimizing the following objective function given in (4).

$$J_w = \left\{ \sum_{t=t_1}^{t_f} [G(t+1) - \hat{G}(t+1|t, w)]^2 \right\} \quad (4)$$

In this study, we assumed new measurement is available in the half-time of prediction horizon (e.g., 30-min-ahead prediction is updated at 15-min with a new measurement).

### 3.2 Quantification of model prediction accuracy

An inherent difficulty in quantifying model prediction accuracy is choosing the indexes. Therefore, in this work, we used four indexes which were used in the literatures or used by physicians to quantify the performance of the blood glucose control.

The first index is the Clarke error grid analysis (CEG). (Clarke, 2005) As shown in Fig. 3, each prediction-reference concentration value pair falls into one of five zones, labelled A-E. Especially, the data pair falling into Zone A is considered clinically accurate.

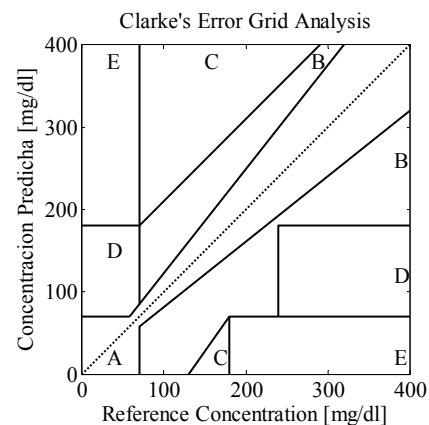


Fig. 3. The Clarke error grid (CEG).

The second index is the FIT which is a statistic metric explained by the model prediction:

$$\text{FIT} = \left(1 - \frac{\|G(t) - \hat{G}(t)\|}{\|G(t) - \bar{G}(t)\|}\right) \times 100\% \quad (5)$$

where  $G(t)$  is the vector of CGMS data,  $\hat{G}(t)$  is the model predicted glucose, and  $\bar{G}(t)$  is the mean of  $G(t)$ .

Moreover, there exists another index for stressing the importance of ignoring the outlier error. This index is the median relative absolute difference (MRAD), the relative absolute difference (RAD) is shown in (6), and MRAD is the median of RAD.

$$\text{RAD}(t) = \frac{|G(t) - \hat{G}(t)|}{G(t)} \times 100\% \quad (6)$$

Another index is the sum of squares of the glucose prediction error (SSGPE) corresponding to the normalized SSE, and this index can be referred when compared with other research results.

$$\text{SSGPE} = \sqrt{\frac{\sum (G(t) - \hat{G}(t))^2}{\sum G(t)^2}} \times 100\% \quad (7)$$

## 4. CASE STUDY

### 4.1 The identification of the HWM

The subject with type 1 diabetes (female, 55 kg, BMI 20 kg/m<sup>2</sup>) was treated by the CSII therapy in this study. The meal contents and insulin dosages were recorded, and the blood glucose measurements were collected by the CGMS (Medtronic Minimed, Northridge, CA) for three days during the experiment period. No special arrangement was made and this patient was asked to live in her normal way with meals and work as usual. The rapid acting insulin analogue Aspart was used by an insulin pump in this experiment, as well as we applied the HWM to this real patient. Based on our abovementioned procedures, the detailed information of the identified HWM is shown in Fig. 4. Next, we excited this identified HWM to generate sufficient data for the SRNNM training.

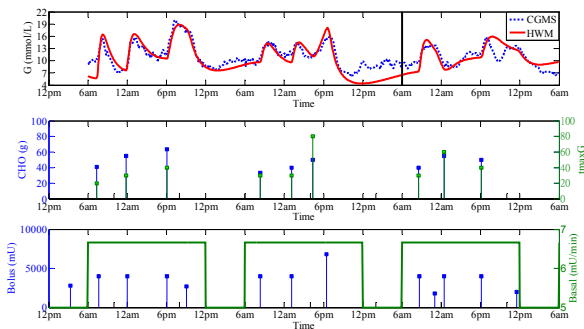


Fig. 4. The results of the HWM identification.

### 4.2 Structured RNN model simulation

In this work, the SRNNM was simulated using the Matlab neural network toolbox. For each sub-RNN in this model, we employed the feed-forward back-propagation network with one hidden layer. The data set which contained three days measurements was divided into two parts. The first part consisting of two days of the data set was used to identify and train the networks (i.e., training set), and the other part called validation set contained one day of the data set. In addition, the Levenberg-Marquardt algorithm (LM) was used to optimize the mean square error (MSE), that is, the quantitative measure of the performance. This LM optimization method was selected because the learning rate was faster than the classical back-propagation algorithm, and the early stopping strategy was adopted for improving generalization. Several experiments were conducted with the purpose of choosing the appropriate number of neurons in the hidden layer. This number in each network was determined as 19, 23, 27, 28, 15, and 22, for  $q_3$ ,  $x_1$ ,  $x_2$ ,  $x_3$ ,  $Q_1$  and  $Q_2$  respectively, because there was no significant decrease of the MSE when we evaluated this error by further varying the number of neurons. Finally, we used the data from the HWM to train the off-line SRNNM and forecasted the BG levels by the on-line recursive prediction.

### 4.3 Model prediction results

The results of the SRNNM for each prediction horizon are shown in Fig. 5, and Tables 1 and 2 display the quantification of accuracy based on CEG Zone A value, FIT value, MRAD value, SSGPE value. As shown in Table 1, for 30-min-ahead prediction employed our proposed structured RNN model, the overall CEG Zone A value, FIT value, MRAD value and SSGPE value are 98%, 72.3%, 4.4% and 6.7% respectively. For the longer prediction horizons (2-hr-ahead, 4-hr-ahead), the values provided in Table 1 reveal the performances still have significant accuracy, for example, for the 4-hr-ahead prediction horizon, the overall CEG Zone A value, FIT value, MRAD value, and SSGPE value, are 90%, 58.6%, 5.5%, and 10.1%, respectively.

To compare the quantification accuracy of the updated prediction results with the aforementioned results, the promising results shown in Table 2 can be seen that there are significant improvements for this available measurement update scheme applied for our purposed model. For instance, for the 30-min-ahead prediction horizon shown in Table 2, the overall CEG Zone A value, FIT value, MRAD value, SSGPE value are 100%, 80.9%, 2.8%, 4.6%, respectively. In summary, those aforementioned results indicate that our purposed SRNNM still has significant accuracy even though we need to forecast for the longer prediction horizon, as well as this model is more accurate when we use new available measurements to update predictive BG.

## 4. DISCUSSION AND CONCLUSIONS

The results derived from this investigation indicate that the prediction of BG levels for the patients with T1DM is possible. To compare with two relevant research papers, firstly, the paper proposed by Bellazzi et al. (1995) is focused

on implementation of a mathematical model for the simulation of a patient with T1DM, identification using neural networks, and performing simulation studies on closed-loop control. By contrast, we try to clarify and solve the problems for a real patient with T1DM. Secondly, Mougiakakou et al. (2005) developed a simulation model but validated by the data from invasive finger lacing test instead of the CGMS data which can provide maximal information about BG levels. Therefore, the authors may neglect the masked BG concentrations between two available measurements. On the other hand, they only identified and validated their model, but didn't test the performance of long-term prediction.

A structured recurrent neural network model has been presented, and this model uses a real patient's CGMS data for identification and validation. By using the HWM to generate sufficient data, our developed neural network model can be realized. Moreover, there exists an obvious advantage. We can use those sufficient data to avoid model overfitting, which is an inherent problem in training neural network model, for improving generalization. After constructing the framework of the model, we test the on-line prediction performance of this model for practical purpose. Finally, in model prediction results section, the promising performance is shown; therefore, we could anticipate the improvement of insulin therapies by using our developed model in our future works.

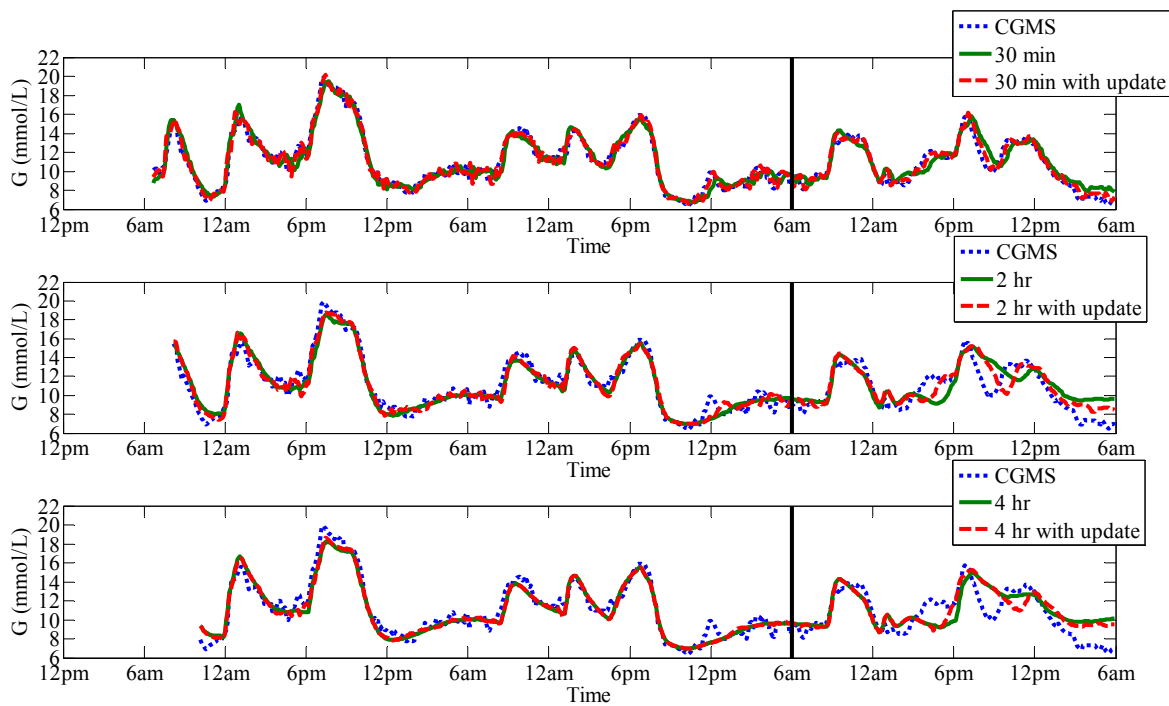


Fig. 5. The results of prediction by the SRNNM for each prediction horizon. ( $\hat{y}(t|t-N)$  v.s.  $y(t)$ )

**Table 1. Quantification of accuracy for each prediction horizon of the structured RNN model without update**

Prediction n horizons	CEG (%)	FIT (%)	MRAD (%)	SSGPE (%)
30min	98	72.3	4.4	6.7
2 hr	91	60.1	5.4	9.7
4 hr	90	58.6	5.5	10.1

**Table 2. Quantification of accuracy for each prediction horizon of the structured RNN model with update**

Prediction n horizons	CEG (%)	FIT (%)	MRAD (%)	SSGPE (%)
30min	100	80.9	2.8	4.6
2 hr	93	65.2	5.0	8.4
4 hr	90	60.1	5.5	9.7

REFERENCES

BELLAZZI, R., SIVIERO, C., STEFANELLI, M. & DE NICOLAO, G. 1995. Adaptive controllers for intelligent monitoring. *Artif Intell Med*, 7, 515-40.

BERGMAN, R. N. 2003. The minimal model of glucose regulation: a biography. *Adv Exp Med Biol*, 537, 1-19.

BOLIE, V. W. 1961. COEFFICIENTS OF NORMAL BLOOD GLUCOSE REGULATION. *Journal of Applied Physiology*, 16, 783-&.

CLARKE, W. L. 2005. The original Clarke Error Grid Analysis (EGA). *Diabetes Technol Ther*, 7, 776-9.

FINAN, D. A., PALERM, C. C., DOYLE, F. J., SEBORG, D. E., ZISSER, H., BEVIER, W. C. & JOVANOVIC, L. 2009. Effect of Input Excitation on the Quality of Empirical Dynamic Models for Type 1 Diabetes. *Aiche Journal*, 55, 1135-1146.

HOVORKA, R., CANONICO, V., CHASSIN, L. J., HAUETER, U., MASSI-BENEDETTI, M., FEDERICI, M. O., PIEBER, T. R., SCHALLER, H. C., SCHAUPP, L., VERING, T. & WILINSKA, M. E. (2004) Nonlinear model predictive control of glucose concentration in subjects with type 1 diabetes. *Physiological Measurement*, 25, 905-920.

MAN, C. D., RIZZA, R. A. & COBELLI, C. 2007. Meal simulation model of the glucose-insulin system. *Ieee Transactions on Biomedical Engineering*, 54, 1740-1749.

MOUGIAKAKOU, S. G., PROUNTZOU, K. & NIKITA, K. S. Year. A Real Time Simulation Model of Glucose-Insulin Metabolism for Type 1 Diabetes Patients. In: *Engineering in Medicine and Biology Society, 2005. IEEE-EMBS 2005. 27th Annual International Conference of the, 2005.* 298-301.

SORENSEN, JOHN THOMAS. "A PHYSIOLOGIC MODEL OF GLUCOSE METABOLISM IN MAN AND ITS USE TO DESIGN AND ASSESS IMPROVED INSULIN THERAPIES FOR DIABETES". S.C.D.C. diss., Massachusetts Institute of Technology, 1985. In *Dissertations & Theses: A&I* [database on-line]; available from <http://www.proquest.com> (publication number AAT 0373597; accessed April 21, 2010).

TOFFOLO, G., BERGMAN, R. N., FINEGOOD, D. T., BOWDEN, C. R. & COBELLI, C. 1980. Quantitative estimation of beta cell sensitivity to glucose in the intact organism: a minimal model of insulin kinetics in the dog. *Diabetes*, 29, 979-90.

TRAJANOSKI, Z. & WACH, P. 1998. Neural predictive controller for insulin delivery using the subcutaneous route. *Ieee Transactions on Biomedical Engineering*, 45, 1122-1134.

TRESP, V., BRIEGEL, T. & MOODY, J. (1999) Neural-network models for the blood glucose metabolism of a diabetic. *Ieee Transactions on Neural Networks*, 10, 1204-1213.

WILINSKA, M. E., CHASSIN, L. J., SCHALLER, H. C., SCHAUPP, L., PIEBER, T. R. & HOVORKA, R. (2005) Insulin kinetics in type-1 diabetes: Continuous and bolus delivery of rapid acting insulin. *Ieee Transactions on Biomedical Engineering*, 52, 3-12.

Appendix A. HOVORKA-WILLINSKA MODEL

$$\frac{dQ_1(t)}{dt} = -\left[\frac{F_{01}^c}{V_G G(t)} + x_1(t)\right]Q_1(t) + k_{12}Q_2(t) - F_R + U_G + W \cdot EGP_0[1 - x_3(t)] \quad (8)$$

$$\frac{dQ_2(t)}{dt} = x_1(t)Q_1(t) - [k_{12} + x_2(t)]Q_2(t) \quad (9)$$

$$G(t) = Q_1(t) / V_G \quad (10)$$

$$F_{01}^c = \begin{cases} F_{01} \cdot W & G \geq 4.5 \text{ mmol/L} \\ F_{01} \cdot W \cdot G(t) / 4.5 & \text{otherwise} \end{cases} \quad (11)$$

$$F_R = \begin{cases} 0.003[G(t) - 9]V_G \cdot W & G \geq 9 \text{ mmol/L} \\ 0 & \text{otherwise} \end{cases} \quad (12)$$

$$U_G = \sum_{i=1}^N \frac{D_G A_G (t - T_i) e^{-\frac{(t-T_i)}{t_{\max,G}^2}}}{t_{\max,G}^2} S(t - T_i) \quad (13)$$

$$\frac{dx_1(t)}{dt} = -k_{a1}x_1(t) + \frac{k_{a1}S_{IR}^f q_3}{WV_1} \quad (14)$$

$$\frac{dx_2(t)}{dt} = -k_{a2}x_2(t) + \frac{k_{a2}S_{ID}^f q_3}{WV_1} \quad (15)$$

$$\frac{dx_3(t)}{dt} = -k_{a3}x_3(t) + \frac{k_{a3}S_{IE}^f q_3}{WV_1} \quad (16)$$

$$\frac{dq_{1a}(t)}{dt} = ku - k_{a1^*}q_{1a}(t) - \frac{V_{\max,LD}q_{1a}(t)}{(k_{M,LD} + q_{1a}(t))} \quad (17)$$

$$\frac{dq_{1b}(t)}{dt} = (1 - k)u - k_{a2^*}q_{1b}(t) - \frac{V_{\max,LD}q_{1b}(t)}{(k_{M,LD} + q_{1b}(t))} \quad (18)$$

$$\frac{dq_2(t)}{dt} = k_{a1^*}q_{1a}(t) - k_{a1^*}q_2(t) \quad (19)$$

$$\frac{dq_3(t)}{dt} = k_{a1^*}q_2(t) + k_{a2^*}q_{1b}(t) - k_e q_3(t) \quad (20)$$